

Critical field of a superconductor—normal-metal—superconductor junction

D. F. Cowen, M. I. Hartzell, M. P. Zaitlin,* and W. E. Lawrence

Dartmouth College, Hanover, New Hampshire 03755

(Received 27 January 1984)

We have computed the lower critical field H_{c1} of a superconductor—normal-metal—superconductor sandwich as a function of normal-metal thickness. The Ginzburg-Landau free-energy functional is minimized by varying the order parameter while computing the magnetic field exactly by numerical means. Good agreement with Pb-Cd sandwiches is found with no adjustable parameters. Comparison is also made with a previous calculation of H_{c1} for the large-thickness limit.

I. INTRODUCTION

A superconductor—normal-metal—superconductor (SNS) junction is one of the simplest inhomogeneous superconducting systems and it has received much theoretical and experimental attention. For this reason we begin our study of the critical magnetic field and magnetic flux entry into inhomogeneous materials with an investigation of the critical field of an SNS junction. Not only is this system better characterized than most inhomogeneous materials but there also exists experimental data in the literature.

In an SNS junction the middle normal layer exhibits a Meissner state at low fields due to the proximity effect from the neighboring superconducting layers. At some critical field H_{c1} this Meissner state is destroyed and magnetic flux enters the junction, usually in the form of a linear array of quantized vortices which are entirely or at least primarily localized within the normal layer.

A calculation of this critical field was first carried out by Dobrosavljevic and de Gennes¹ (DG). Their calculation used the variational principle to determine H_{c1} , by assuming a reasonable analytic form for the magnetic field of the vortex. In order for their functional form of the magnetic field to be valid, the vortex had to be wholly contained within the normal metal and this (as well as several other approximations) made the calculation valid only for normal-state thicknesses which are large compared to the coherence length in the normal metal. Within this approximation it was found that

$$H_{c1} = \{ \Phi_0 / 8\lambda_B [\xi_n(a_n - \rho)]^{1/2} \cosh(a_n / \xi_n) \}, \quad (1)$$

where Φ_0 is the flux quantum, $2a_n$ the normal-metal thickness, ξ_n the coherence length in the normal metal, λ_B the effective penetration depth in the normal metal at the superconducting—normal-metal boundary, and ρ is defined as $\xi_n [\ln(0.89\xi_n / \lambda_B)]$, which is typically a few times the coherence length. The unphysical divergence at a thickness $a_n = \rho$ is the result of approximations made in the calculation and emphasizes the large-thickness approximation of the result. This restriction means in practice that Eq. (1) is useful only when H_{c1} is less than 10^{-2} – 10^{-3} of the critical field of the superconductor.

For a typical superconductor such as Pb this corresponds to H_{c1} less than a few gauss.

In this paper we describe a calculation of H_{c1} for arbitrary thickness of normal metal. This requires treating the vortex-core explicitly, and also allowing for magnetic field penetration into the superconductor. The vortex-core shape is determined by a variational solution of the appropriate Ginzburg-Landau equation; this parallels Clem's treatment² of H_{c1} in a homogeneous superconductor. The magnetic field is then computed by integrating numerically the second Ginzburg-Landau equation. We find that for a range of material parameters the calculated H_{c1} has a very simple functional form. In addition we make comparison to experimental data on a Pb-Cd lamellar eutectic composite and find good agreement with no adjustable parameters.

II. TREATMENT OF THE GINZBURG-LANDAU EQUATIONS

We begin by writing the Ginzburg-Landau equations for the order parameter ψ and magnetic field $\vec{H} = \vec{\nabla} \times \vec{A}$ in the usual way,³

$$\alpha\psi + \beta |\psi|^2\psi + \frac{1}{2m^*} \left[\frac{\hbar}{i} \vec{\nabla} - \frac{e}{c} \vec{A} \right]^2 \psi = 0, \quad (2)$$

$$\vec{j} = \frac{c}{4\pi} \vec{\nabla} \times \vec{H} = \frac{e^* \hbar}{2m^* i} (\psi^* \vec{\nabla} \psi - \psi \vec{\nabla} \psi^*) - \frac{(e^*)^2}{m^* c} |\psi|^2 \vec{A}, \quad (3)$$

where in our case the parameters α and β are piecewise constant functions of position taking on values $\alpha_s < 0$, and $\beta_s > 0$ in the superconductor, and $\alpha_n > 0$, $\beta_n > 0$ in the normal layer. The lower critical field H_{c1} is given by the difference between the Helmholtz free energies (per unit length) of the one-vortex and no-vortex states,⁴

$$H_{c1} = \frac{4\pi}{\Phi_0} \int d^2r [\mathcal{F}_1(\vec{r}, \vec{H}(\vec{r})) - \mathcal{F}_0(\vec{r})], \quad (4)$$

where \mathcal{F}_1 is the density

$$\mathcal{F}_1(\vec{r}, \vec{H}(\vec{r})) = \alpha |\psi|^2 + \frac{\beta}{2} |\psi|^4 + \frac{\hbar^2}{2m^*} (\vec{\nabla} |\psi|)^2 + \frac{m^*}{2} \left[\frac{c |\vec{\nabla} \times \vec{H}|}{4\pi e^* |\psi|} \right]^2 + \frac{1}{8\pi} H^2 \quad (5)$$

in the presence of a single vortex [for which $\int d^2r H(\vec{r}) = \Phi_0$], and \mathcal{F}_0 is given by the same expression with $H=0$.

At fixed magnetization, the solutions of (2) and (3) minimize the Helmholtz free energy. In our case where quantities do not vary in the direction (z) of the magnetic field, one essentially minimizes the free energy per unit length $\int d^2r \mathcal{F}(\vec{r}, \vec{H}(\vec{r}))$ at constant magnetic flux $\int d^2r H(\vec{r})$.

$$g(x) = \begin{cases} \tanh(b/\sqrt{2}\xi_s) \cosh(x/\xi_n) / \cosh(a_n/\xi_n), & |x| \leq a_n \\ \tanh\left[\frac{|x| + b - a_n}{\sqrt{2}\xi_s}\right], & |x| > a_n \end{cases} \quad (6b)$$

where the coherence lengths $\xi_{s,n}$ in the superconducting and normal metals are given by

$$\xi_s^2 = \hbar^2 / 2m^* |\alpha_s|, \quad \xi_n^2 = \hbar^2 / 2m^* \alpha_n \quad (7)$$

and b is chosen so that g' as well as g is continuous at $x = \pm a_n$. In the presence of a singly-quantized vortex, we may choose $\psi(\vec{r}) = |\psi(\vec{r})| e^{i\phi}$ [where $\phi = \tan^{-1}(y/x)$; this is completely general owing to gauge invariance], and utilize the variational principle to approximate $|\psi(r)|$. We assume that the vortex-induced distortions of $|\psi|$ have cylindrical symmetry, corresponding to the variational function,

$$\psi_1(\vec{r}) = \psi_\infty g(x) f(r) e^{i\phi}, \quad (8a)$$

where f has the form suggested by Clem,²

$$f(r) = r(r^2 + \xi_v^2)^{-1/2}, \quad (8b)$$

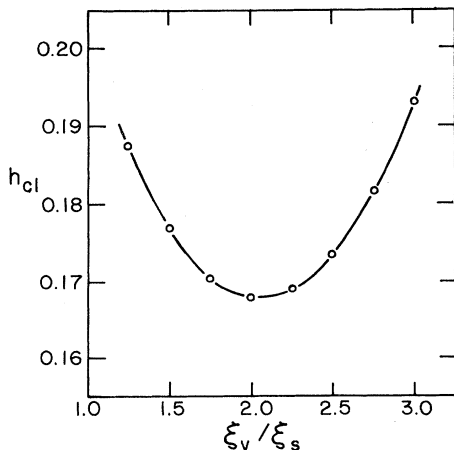


FIG. 1. Reduced critical field versus normalized variational parameter for parameters $\kappa_s=5.0$, $\kappa_n=0.2$, $\xi_n/\xi_s=10$, $2a_n/\xi_n=1.08$.

If we know the zero-field solution $\psi_0(x,y)$ exactly, then H_{c1} [Eq. (4) with the exact \mathcal{F}_0] may be regarded as a functional of the single-vortex functions ψ_1 and H [where $\int d^2r H(\vec{r}) = \Phi_0$]. The minimum value of H_{c1} is achieved only if ψ_1 and H are the solutions of (2) and (3).

We first consider the zero-field solution [of Eq. (2)], and write this as

$$\psi_0(x) = \psi_\infty g(x), \quad (6a)$$

where x is perpendicular to the normal layer, and ψ_∞ is the value of ψ deep within the superconductor, so that $g \rightarrow 1$ as $|x| \rightarrow \infty$. If we put $\beta_n=0$, then the solution may be written in a simple form. With the normal-metal–superconductor (NS) boundaries at $\pm a_n$, we have

and H_{c1} is to be minimized with respect to ξ_v . Clem² has shown that this is an excellent approximation for a bulk superconductor, with the optimal ξ_v being comparable to ξ_s . One then expects (8b) to be a good approximation for the thin normal layers. In the opposite limit of thick layers the details of $f(\vec{r})$ should be unimportant.

As expected, the calculation yields a fairly broad minimum in H_{c1} as a function of ξ_v as can be seen in Fig. 1. Typically a 10% error in ξ_v caused less than a 1% error in H_{c1} . Figure 2 shows the optimal values of ξ_v for several different values of the material parameters. For small a_n/ξ_n , ξ_v has a value close to that expected for a bulk superconductor. At larger values of a_n/ξ_n , ξ_v approaches ξ_n and then decreases at still larger a_n .

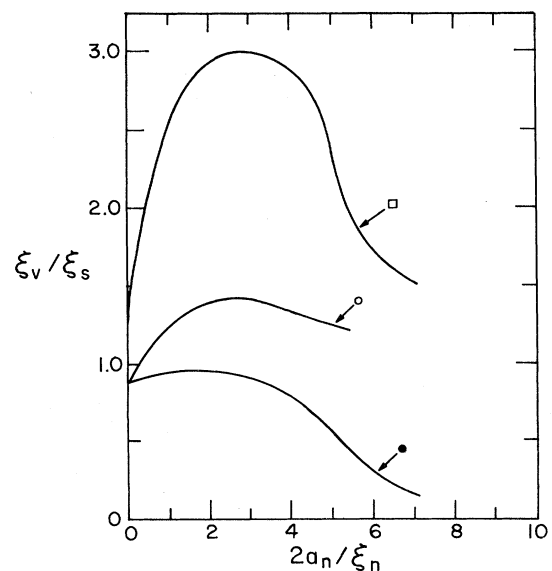


FIG. 2. Normalized variational parameter versus normalized normal-metal thicknesses: ●, $\kappa_s=0.5$, $\kappa_n=0.2$, $\xi_n/\xi_s=1$; ○, $\kappa_s=0.5$, $\kappa_n=0.067$, $\xi_n/\xi_s=3$; □, $\kappa_s=5.0$, $\kappa_n=0.2$, $\xi_n/\xi_s=10$.

Once ψ is specified according to Eqs. (8), the magnetic field equation (3) simplifies to

$$\lambda_s^2 \vec{\nabla} \times [(gf)^{-2} \vec{\nabla} \times \vec{H}] + \vec{H} = \hat{z} \Phi_0 \delta^2(\vec{r}), \quad (9)$$

where the penetration depth in the bulk superconductor is given as usual by $\lambda_s^2 = m^* c^2 / (4\pi e^2 \psi_\infty^2)$. A local effective penetration depth may be defined formally by $\lambda(x) = \lambda_s \psi_\infty |\psi(\vec{r})|^{-1} = \lambda_s (gf)^{-1}$, although the concept is not well defined if $|\psi|$ varies sufficiently rapidly. We solve Eq. (9) numerically on a mesh which is defined to precisely locate the NS boundary, and also to adequately describe the vortex-core region. The method is described in the Appendix.

It is useful in the SNS geometry (as well as in the homogeneous case) to characterize a superconductor not by λ_s but by the ratio $\kappa_s = \lambda_s / \xi_s$, since this parameter determines whether one has type-I or type-II behavior. From this (usual) definition one may deduce that $\kappa_s^2 \sim \beta_s$. The latter relation suggests a useful definition of κ_n for the normal metal, where there is no intrinsic penetration depth:

$$\kappa_{s,n}^2 = \frac{1}{2\pi} \left[\frac{m^* c}{e^* \hbar} \right]^2 \beta_{s,n}. \quad (10)$$

Thus our system is characterized by the width of the normal layer $2a_n$ and (within Ginzburg-Landau theory) by material parameters $\kappa_{s,n}$ [Eq. (10)] and $\xi_{s,n}$ [Eq. (7)]. The superconductor's parameters may be determined empirically from the temperature-dependent penetration depth and the thermodynamic critical magnetic field,³

$$h_{c1} = \frac{\kappa_s}{4\pi} \int d^2 \rho \Delta \mathcal{L}, \quad (14a)$$

$$\Delta \mathcal{L} = h^2 + 2(gf)^{-2} \left[\left(\frac{\partial h}{\partial x} \right)^2 + \left(\frac{\partial h}{\partial y} \right)^2 \right] + \left[\text{sgn}(\alpha) (\xi_s / \xi)^2 g^2 + \kappa_s^{-2} \left(\frac{\partial g}{\partial x} \right)^2 + \frac{1}{2} (\kappa / \kappa_s)^2 g^4 (f^2 + 1) \right] (f^2 - 1) + \kappa_s^{-2} g \frac{\partial f}{\partial \rho} \left[g \frac{\partial f}{\partial \rho} + 2(x/\rho) f \frac{\partial g}{\partial x} \right], \quad (14b)$$

where ξ and κ (without subscripts) refer to the local values. (Dimensionless coordinates are $x = x/\lambda_s$ and $y = y/\lambda_s$.)

III. RESULTS AND DISCUSSION

The results of our calculations for several values of the material parameters are shown in Fig. 3. Changing the coherence length in the normal or in the superconducting material does not change the exponential behavior of the reduced field over a wide range of parameters. In fact, the data shown here are well represented by the equation

$$h_{c1}(a_n) = h_{c1}(0) e^{-\gamma a_n / \xi_n}, \quad (15)$$

where $h_{c1}(0)$ is the reduced critical field for the homogeneous superconductor and γ is a constant ≈ 1.2 . This exponential behavior is not totally unexpected since it is similar to that predicted by DG. Additionally if one were

$$\kappa_s = \lambda_s / \xi_s = 2\pi \sqrt{2} H_c \lambda_s^2 / \Phi_0. \quad (11)$$

For the normal metal we must appeal to arguments such as the following: If there is no interaction between electrons in the normal metal and the mean-free path is long, then the coherence length is⁵

$$\xi_n = \hbar v_F / 2\pi k_B T \quad (12)$$

and $\kappa_n = 0$, corresponding to no nonlinear term in the microscopic gap equation. In the more complicated situation where the normal metal becomes superconducting at some T_{cn} (where $0 < T_{cn} < T$), microscopic calculations^{5,6} suggest that Eq. (12) is still a good approximation (as long as T is not too close to T_{cn} where ξ_n diverges). As for κ_n , the usual derivation of the Ginzburg-Landau equations⁷ suggests that κ_n is a constant, equal to its value just below T_{cn} . Of course the Ginzburg-Landau equations cannot be justified microscopically in our situation,⁸ and so we view this calculation as a test of their usefulness.

The two basic equations needed for our remaining discussion may be usefully rewritten in terms of the four parameters just discussed. We rewrite Eq. (9) in terms of the dimensionless distance $\vec{r} = \vec{r}/\lambda_s$ and the reduced magnetic field $\vec{h} = \vec{H}/\sqrt{2}H_c$. With the use of Eq. (11), the result is

$$\vec{\nabla} \times [(gf)^{-2} \vec{\nabla} \times \vec{h}] + \vec{h} = \frac{2\pi}{\kappa_s} \hat{z} \delta^2(\vec{r}). \quad (13)$$

The reduced critical field $h_{c1} = H_{c1}/\sqrt{2}H_c$ then appears [from Eqs. (4) and (5)] as

to make a reasonable guess that h_{c1} was proportional to the value of the order parameter at the center of the normal metal, then for large a_n one would have $h_{c1} \sim 1/\cosh(a_n/\xi_n) \sim \exp(-a_n/\xi_n)$. At small a_n there would also be exponential decay but with a different decay constant. What is surprising is that the calculation shows the same exponential decay constant in both limits for a range of material parameters. (We shall return to this point later.) For $a_n \rightarrow 0$, this calculation reproduces the h_{c1} of a homogeneous superconductor to within a few percent, as expected since in that limit we are simply reproducing the calculation of Clem.²

For the case of $\kappa_s = 0.5$, the superconducting material is type I which is reflected in the calculation as a reduced critical field greater than $1/\sqrt{2}$, for small reduced thickness (i.e., $a_n \ll \xi_n$ near 0). Here vortices are thermodynamically unfavorable at all fields less than H_c of the superconductor. Of course for sufficiently large a_n we can always find $h_{c1} < 1/\sqrt{2}$ so that type-II behavior occurs. A

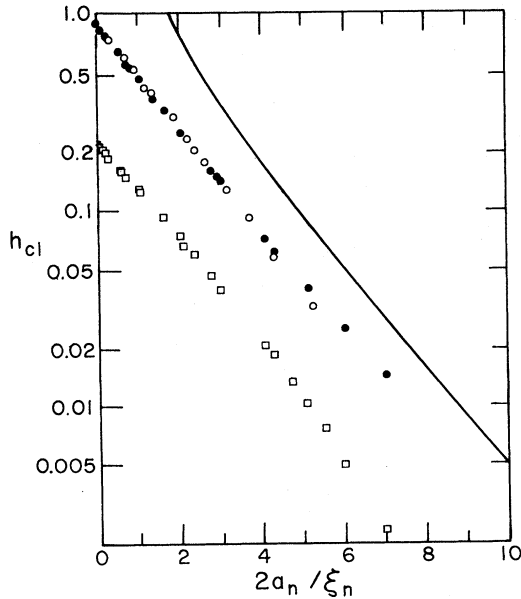


FIG. 3. Reduced critical field versus normalized normal-metal thickness for several values of material parameters: ●, $\kappa_s=0.5$, $\kappa_n=0.2$, $\xi_n/\xi_s=1$; ○, $\kappa_s=0.5$, $\kappa_n=0.067$, $\xi_n/\xi_s=3$; □, $\kappa_s=5.0$, $\kappa_n=0.2$, $\xi_n/\xi_s=10$. The solid line corresponds to the DG formula [Eq. (17)], evaluated for parameters corresponding to ●.

transition from type-I to type-II behavior occurs at some critical thickness a_{nc} which, if Eq. (15) holds, is

$$a_{nc} = \frac{\xi_n}{\gamma} \ln[\sqrt{2}h_{c1}(0)], \quad (16)$$

or roughly $a_{nc} = 0.7\xi_n$ for the case of $\kappa_s = 0.5$. The physical critical thickness is temperature dependent since ξ_n is, but the transition is always present if the superconducting material is type I.

Initially it was thought that increasing the Ginzburg-Landau parameter of the superconductor κ_s might lower the zero-thickness critical field $h_{c1}(0)$ below that for a finite thickness. No such positive slope in h_{c1} versus a_n was observed. Increasing κ_s reduced the critical fields at all values of a_n .

To compare our results with those of DG we need an expression for λ_B [in Eq. (1)] in terms of our parameters. This can be found by noting that DG define the local penetration depth corresponding to our expression $\lambda_s(gf)^{-1}$ in Eq. (9), and hence λ_B is this expression evaluated at $x = \pm a_n$. For parameters in the range studied here, this is close to λ_s , which leads to

$$h_{c1}^{DG} = \frac{(\pi/4)(\xi_s/\xi_n)}{[a_n/\xi_n - \ln(0.89\xi_n/\kappa_s\xi_s)]^{1/2} \cosh(a_n/\xi_n)}. \quad (17)$$

This expression is compared to our calculation in Fig. 3. Both calculations show a similar nearly exponential behavior and differ primarily in their prefactors. While the numerical calculation cannot predict the behavior at thicknesses larger than those shown, it is known to give

the correct result in the limit of zero thickness—whereas an extrapolation of the DG result from large a_n , assuming the same exponential behavior is valid, would give an incorrect result for the zero-thickness limit.

The form of Eq. (15) suggests that h_{c1} is independent of κ_n , and this is true at least for small κ_n as shown in Fig. 4. For the range of parameters studied here it would appear that whether or not Eq. (15) holds depends on the relative magnitudes of λ_s and λ_n , where the latter is a purely formal definition $\kappa_n\xi_n$. For $2a_n/\xi_n \sim 2$ as seen in Fig. 4 it appears that the range of validity for Eq. (15) is given roughly by $\lambda_n/\lambda_s \lesssim 1$. The effect of the relative sizes of λ_s and λ_n on h_{c1} can be seen in Fig. 5. The curve with $\lambda_n = 0.8\lambda_s$ is close to exponential as expected, while the curve with $\lambda_n = 2\lambda_s$ is exponential but with a steeper slope for small a_n and then no longer exponential at larger thicknesses. The amusing thing about these two cases is that only ξ_n (of the four Ginzburg-Landau parameters $\xi_{s,n}$ and $\kappa_{s,n}$) differs appreciably from one case to the other. Nevertheless the two curves differ (theoretically, at least) only because $\kappa_n \neq 0$, i.e., the difference arises from the nonlinear term of the Ginzburg-Landau equation in the normal metal.

That this effect should be signaled by the combination λ_n/λ_s (Fig. 4) is suggested by examining the expression for free-energy density [Eq. (14b)]; the ratio of coefficients of the g^4 and g^2 terms in the normal metal is just λ_n^2/λ_s^2 . For small thicknesses $g(x)$ is never much less than unity, and so $\partial^2 g/\partial x^2$ is approximately $\xi_n^{-2}(1 + \lambda_n^2/\lambda_s^2)$. (Here x is the physical distance $\lambda_s x$.) Thus we would expect the initial slope of $\ln h_{c1}$ versus a_n/ξ_n to be increased in magnitude by $(1 + \lambda_n^2/\lambda_s^2)^{1/2}$. For large thicknesses, on the other hand, $g(x)$ is small over most of the region of the normal metal. One might expect in this limit that the nonlinear effect would be revealed by changing the effective thickness $2a_n$ by some constant amount, rather than by changing the effective normal-metal coherence length

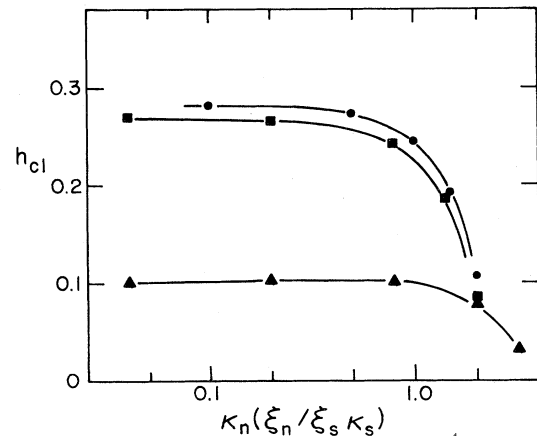


FIG. 4. Reduced critical field versus κ_n times the constant scale factor $(\xi_n/\xi_s\kappa_s)$ which is equivalent to λ_n/λ_s : ●, $\kappa_s=0.5$, $\xi_n/\xi_s=5$; ■, $\kappa_s=0.5$, $\xi_n/\xi_s=2$; ▲, $\kappa_s=2.5$, $\xi_n/\xi_s=10$. For all cases $2a_n/\xi_n \sim 2$.

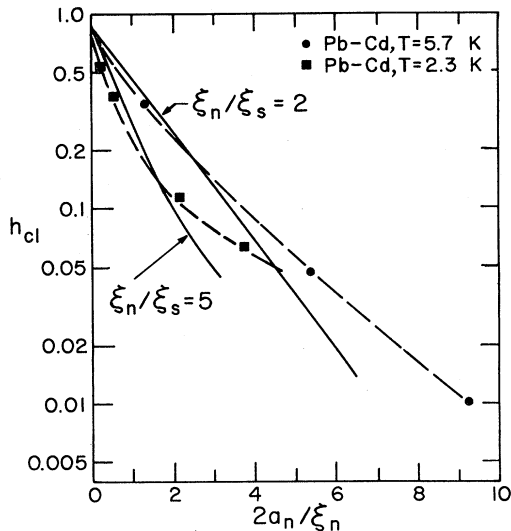


FIG. 5. Reduced critical field versus normalized normal-metal thickness. The \bullet and \blacksquare are for data on Pb-Cd eutectic composites at two different temperatures. The solid lines are calculated results using the material parameters described in the text which should closely correspond to those of Pb and Cd.

ξ_n (i.e., $\ln h_{c1}$ would be reduced, but have the same slope on Fig. 5 as in the $\kappa_n=0$ limit). Our computed results are not sufficiently accurate at large a_n to confirm this expectation. In fact, our approximation of calculating $g(x)$ with $\kappa_n=0$ is not accurate when both a_n and λ_n/λ_s are larger than shown in Fig. 5. We find that eventually h_{c1} becomes negative—a physical impossibility which indicates that our zero-field order parameter is not sufficiently accurate.

We have made a comparison of our calculations with data on a Pd-Cd eutectic composite,⁹ since the critical field in that system has been extensively studied and has parameters which are within the range of our calculations. In addition, that system is formed directly from the melt so it would not be expected to have an oxide barrier or other forms of contamination between layers as can sometimes occur with vapor-deposited films. To make a comparison with the calculations, the experimental data on several annealed samples were interpolated to arrive at the critical field at two fixed temperatures. The critical field was normalized using the known critical field for pure Pb. The normal-metal thickness was normalized using the value $\xi_n=9600/T$ Å (Ref. 9) calculated from Eq. (12).

The data for the higher temperature have a nearly exponential behavior with slightly less than the calculated slope, while the data for the lower temperature are decidedly not exponential. This is similar to the dependence of the calculated curves in the same figure, with the change in behavior due to the difference in relative magnitudes of λ_s and λ_n as explained above. The calculation assumes $\xi_s=830$ Å (Ref. 10) and $\kappa_s=0.5$ for Pb, and $\kappa_n=0.2$ (Ref. 11) with ξ_n as given previously for Cd. With no adjustable parameters the calculation shows very reasonable agreement with the data. No attempt was made to adjust the material parameters to find a better fit to the data.

Equation (15) also provides a qualitative explanation for the temperature dependence of H_{c1} . The primary effect of changing the temperature is to change ξ_n , since the other parameters are less temperature dependent (or less important for H_{c1}). For samples with $a_n \ll \xi_n$ over the temperature range studied, h_{c1} would be nearly constant indicating a temperature dependence of H_{c1} similar to that of H_c (namely, $\propto 1-t^2$) as is seen experimentally. For $a_n > \xi_n$, h_{c1} would have an exponential temperature dependence $\sim \exp(-\gamma a_n 2\pi k_B T / \hbar v_F)$ so that H_{c1} would rise rapidly at low temperature. This is in accord with the observed change in the curvature of $H_{c1}(T)$ from negative to positive as a_n is changed from the thin limit to the thick limit.

ACKNOWLEDGMENT

This work was supported in part by the U.S. Department of Energy through Grant No. DE-AS02-78ER04938.

APPENDIX

The magnetic field is computed by iterating to convergence the finite-difference equation corresponding to Eq. (13). The method of successive over-relaxation is used, which reduces the number of iterations required by up to a factor of 4. To ensure convergence in all cases, we find it necessary to normalize the magnetic field to a single flux quantum following each iteration.

Square meshes are used in order to accurately locate the NS boundary, and the first quadrant of the x - y plane $0 \leq x, y < \infty$ is mapped into the unit square $0 \leq u, v \leq 1$, where

$$u = 1 - e^{-x/a\lambda_s}, \quad (\text{A1})$$

$$v = 1 - e^{-y/a\lambda_s}. \quad (\text{A2})$$

The mesh points are distributed uniformly over the square, and magnetic field differences from point to point are small everywhere. We compute h_{c1} for the sequence of $N \times N$ meshes for which $N=7, 19,$ and 55 . The sequence corresponds to successive reductions by 3 in the interval $\Delta u = \Delta v$ (since points are located at the ends). The factor of 3 is chosen so that if we locate the NS boundary midway between neighboring points in the 7×7 mesh, then it still falls between neighboring points in the finer meshes. Typically, the computed h_{c1} values are very nearly linear in N^{-1} , and may safely be extrapolated to $N^{-1}=0$. Examples are shown in Fig. 6. The extrapolated critical fields are essentially independent of the parameter α over a comfortable range, provided that the width $2a_n$ of the normal layer is not too large. Typically the extrapolation from $N=55$ to ∞ changes h_{c1} by a few percent or less. As the thickness is increased, the most accurate results are obtained with larger α values, but the range of usable values decreases, and the extrapolation becomes less certain. Tolerating at most a 10% change in h_{c1} limits us to thicknesses of about $15\lambda_s$ or less. To consider thicker normal layers we would require a finer mesh.

For purposes of numerical evaluation, we must carefully define the magnetic field at the origin since Eq. (13) has

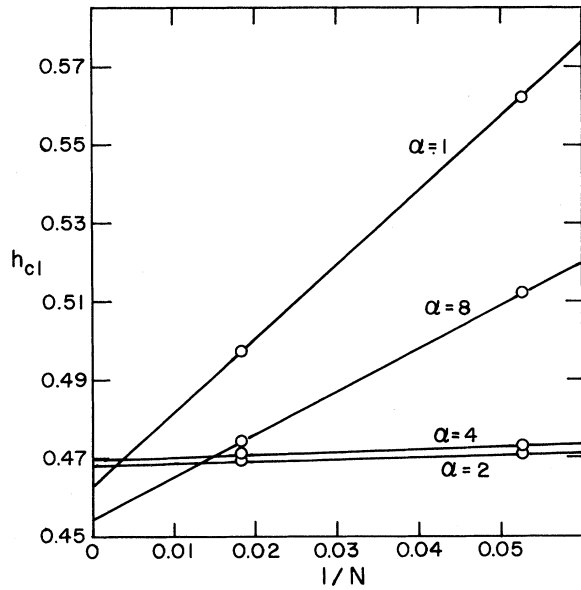


FIG. 6. Calculated reduced critical field versus the reciprocal of the number of points used on the side of the square mesh in the numerical calculation. The calculation for $\alpha=8$ is less accurate due to the reduced number of points within the normal metal.

in its denominator the function $f^2(r)$, which vanishes at $r \rightarrow 0$. It is more convenient then to consider Eq. (3) directly, which appears in terms of our dimensionless variables [introduced with Eq. (13)] as

$$\vec{\nabla} \times \vec{h}(\vec{r}) = g^2(x) f^2(\rho) \left[\frac{\hat{\phi}}{\kappa_s \rho} - \vec{a} \right], \quad (\text{A3})$$

where $\vec{h} = \vec{\nabla} \times \vec{a}$ and $\vec{\nabla}$ is dimensionless. As $\rho \rightarrow 0$, we have $\vec{a} \rightarrow \vec{0}$ and $f(\rho) \rightarrow \rho \lambda_s / \xi_v$, and the resulting limiting behavior of h is

$$\lim_{\rho \rightarrow 0} [h(\vec{r}) - h(\vec{0})] = -\frac{1}{2\kappa_s} [g(0)\lambda_s \rho / \xi_v]^2. \quad (\text{A4})$$

This is used to infer $h(0,0)$ from neighboring points. A similar precaution must be taken when evaluating the free energy density in Eq. (14) for h_{c1} . We evaluate the necessary term by again using (A3):

$$\lim_{\rho \rightarrow 0} \left[\frac{|\vec{\nabla} \times \vec{h}|}{g(x)f(\rho)} \right]^2 = \left[\frac{g(0)\lambda_s}{\kappa_s \xi_v} \right]^2 = \left[\frac{g(0)\xi_s}{\xi_v} \right]^2, \quad (\text{A5})$$

where $|\vec{\nabla} \times \vec{h}|^2$ is written as $(\partial h / \partial x)^2 + (\partial h / \partial y)^2$ in Eq. (14b).

*Present address: Raytheon Corporation, Research Division, Waltham, MA 02154.

¹L. Dobrosavljevic and P. G. de Gennes, *Solid State Commun.* **5**, 177 (1967).

²J. R. Clem, *J. Low Temp. Phys.* **18**, 427 (1975).

³M. Tinkham, *Introduction to Superconductivity* (McGraw-Hill, New York, 1975).

⁴This is equivalent to the statement that the Gibbs free energies $G = F - (4\pi)^{-1} \vec{H}_0 \cdot \int \vec{H} d^3r$ of the one-vortex and no-vortex states are the same, when the external field strength H_0 is equal to H_{c1} .

⁵G. Deutscher and P. G. de Gennes, in *Superconductivity*, edited by R. D. Parks (Dekker, New York, 1969), Vol. 2, p. 1005.

⁶See also T. Y. Hsiang and D. K. Finnemore, *Solid State Commun.* **33**, 847 (1980). They have successfully used a slightly more general formula that exhibits the divergence at T_{cn} , but those numerical values are close to those given by the simpler

expression (12) for T well above T_{cn} as is the case here.

⁷In the spirit of the Ginzburg-Landau approach, we expand the self-consistent equation for the pair potential Δ in powers of Δ . The coefficients of $\partial^2 \Delta / \partial x^2$ and $|\Delta|^2 \Delta$ have the same temperature dependence, so that their ratio $\beta \sim \kappa^2$ is constant. The derivation is valid when Δ is small and slowly varying, but the Ginzburg-Landau equations are frequently used with good results outside this regime (e.g., for T well below T_c). The present study finds good results for T well above T_c .

⁸For a discussion of the microscopic theory of the proximity effect, see W. Silvert, *J. Low Temp. Phys.* **20**, 439 (1975).

⁹M. P. Zaitlin, *Phys. Rev. B* **18**, 3298 (1978).

¹⁰C. Kittel, *Introduction to Solid State Physics*, 5th ed. (Wiley, New York, 1976), p. 376.

¹¹ κ values are computed by taking λ values from T. J. Greytak and J. H. Wernick, *J. Phys. Chem. Solids* **25**, 535 (1964), and ξ values in the superconducting state from Ref. 10.